

GENERATION OF ULTRASHORT LASER PULSES https://doi.org/10.1070/QEL16908

Simulation of generation of ultrashort pulses in a laser based on the nonlinear polarisation evolution in two segments of a polarisation-maintaining fibre

I.N. Bychkov, A.I. Baranov

Abstract. **A model describing generation of ultrashort optical pulses in a fibre cavity with Kerr nonlinearity and normal dispersion is constructed based on numerical solution of a nonlinear Schrödinger equation. The model makes it possible to investigate the specific features of pulsed generation of a passively mode-locked laser based on the effect of nonlinear polarisation evolution (NPE) in two segments of a polarisation-maintaining (PM) fibre. It is shown theoretically that the proposed scheme may provide generation of linearly chirped optical pulses with a spectral width of above 25 nm and a centre wavelength of 1030 nm.**

Keywords: *passive mode locking, ultrashort pulses, nonlinear Schrödinger equation, fibre laser.*

1. Introduction

Generations of ultrashort (shorter than 10 ps) optical pulses is an urgent problem of laser physics. Lasers emitting ultrashort pulses (USPs) are widely used in research, as well as in various technological and medical applications [1–3]. Of particular interest are fibre lasers, which are rather simple in production and highly reliable. Kerr nonlinearity effects are pronounced in single-mode silica fibres, which are actively used for USP generation [4–11].

It is a rather challenging problem to describe theoretically the operation of these lasers. There are two radically different approaches to its solution in the literature. One is based on derivation of a generalised equation, taking into account the influence of all elements of the cavity as a whole, after which its solutions and their specific features are analysed. However, one must apply some essential approximations to construct the desired equation. In particular, an equation describing the pulse propagation in a laser was obtained in [12–15] on the assumption that both nonlinear and dispersion effects, as well as the gain in the active medium are additive and make a small contribution to the laser pulse evolution per cavity round trip. The laser operation was modelled in [16] assuming that a Gaussian pulse propagates in the cavity. The second approach to the simulation of passively mode-locked lasers is based on the numerical solution of a nonlinear Schrödinger equation and calculation of the evolution of some initial pulse, which successively passes through all cavity elements [17–19]. The first approach allows one to see the pulsed laser generation pattern as a whole and to investigate different nonstationary operation regimes. It should be noted that the approximations made when deriving the pulse propagation equation may be inadmissible in many cases, where quantitative rather than qualitative description must be performed. The second approach, which is mathematically more rigorous, allows more exactly the generated pulse parameters to be predicted. However, the computational complexity and amount of necessary computational resources significantly increase in this case. We used specifically this approach to develop the model.

The developed model was used to investigate the operation of a laser passively mode locked due to the nonlinear polarisation evolution (NPE) in a polarisation-maintaining (PM) fibre. Lasers based on this effect have been described in the literature. For example, to implement mode locking, Szczepanek et al. [9] used a segment of a PM fibre, into which linearly polarised radiation with a plane of polarisation making some angle with the slow fibre axis was introduced. Then the radiation arrived at a Faraday mirror to be reflected off with rotation of its polarisation plane by 90°. Thus, the linear polarisation axis of weak radiation at the fibre output is rotated by 90°, and the change in the polarisation state is determined by only the Kerr nonlinearity. If a polariser is placed after the fibre segment, this system forms a nonlinear element, whose transmission depends on the radiation power. A similar scheme with a Faraday isolator is not very suitable for generating pulses with a wide emission spectrum: because of the spectral dependence of the Verdet constant, the rotation angle of the plane of polarisation depends on wavelength, which results in poor polarisation extinction of broadband radiation. As will be shown below, this circumstance is critical for stable laser operation. From this viewpoint, the most optimal approach is to use an additional segment of a PM fibre of the same length, spliced to the first one, with polarisation axes rotated by 90°.

A similar scheme was considered in [19, 20]; however, the operation of only a nonlinear element, in which NPE occurred in three PM fibre segments spliced with rotation of polarisation axes, was investigated in those studies. In this paper, in contrast to [19, 20], we report the results of studying the operation of the entire laser cavity, in which two PM fibre segments served as a nonlinear element.

2. Model

A schematic of a passively mode-locked laser based on the NPE effect in two PM fibre segments is presented in Fig. 1.

I.N. Bychkov, A.I. Baranov NTO IRE-Polus Ltd., pl. Akad. Vvedenskogo 1, stroenie 3, 141190 Fryazino, Moscow region, Russia; Moscow Institute of Physics and Technology (State University), Institutskii per. 9, 141700 Dolgoprudnyi, Moscow region, Russia; e-mail: ilbych12@mail.ru

Received 16 November 2018; revision received 23 February 2019
Kvantovaya Elektronika **49** (8) 762–767 (2019)
Translated by Yu.P. Sin'kov

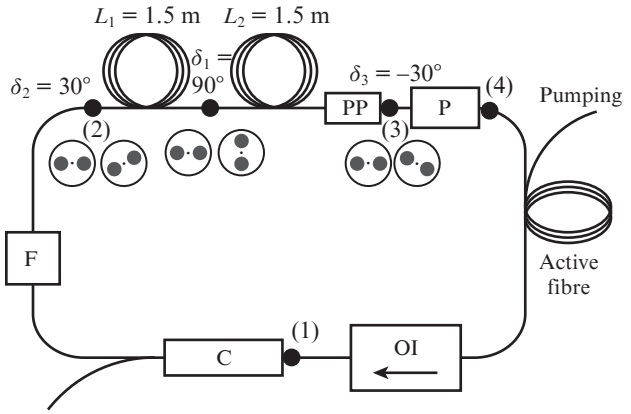

Figure 1. Optical scheme of a laser based on the NPE effect in two PM fibre segments:
(P) polariser blocking the radiation polarised along the fast axis; (OI) optical isolator; (C) coupler; (F) Gaussian spectral filter; (PP) tunable phase plate, coaxial with the PM fibre; and (1)–(4) check points.

An output coupler and an isolator are located after the active optical fibre to provide generation of pulses with maximum energy and spectral width. There is a spectral filter after the output coupler, and the filter is followed by a nonlinear element formed by two PM fibre segments with lengths of L_1 and L_2, spliced with rotation of polarisation axes by an angle of $\delta_1 = 90°$. The simulation was performed on the assumption that $L_1 = L_2$; however, in this case the birefringence effect in the two fibre segments is compensated for, and the polarisation state does not change. To take into account the uncompensated birefringence (i.e., possible difference in L_1 and L_2), a tunable phase plate with an optical axis coinciding with the slow fibre axis was placed after the segment L_2.

The main concept of our model is the calculation of the evolution of a pulse during its transmission through the cavity elements; this approach allowed us to investigate the dependence of generation on any characteristic of the cavity element. In simulating the pulse transmission through the coupler, filter, and isolator, we took into account only the linear loss (with allowance for the spectral dependence). The pulse propagation in passive fibres was computed using a system of nonlinear Schrödinger equations (NSEs), which take into account the dispersion effects up to the third order but disregard Raman self-scattering [21]:

$$\begin{aligned}
&\frac{\mathrm{d}u}{\partial z} + \frac{\Delta\beta_1}{2}\frac{\partial u}{\partial t} + \frac{\mathrm{i}\beta_2}{2}\frac{\partial^2 u}{\partial t^2} - \frac{\beta_3}{6}\frac{\partial^3 u}{\partial t^3} + \frac{\alpha}{2}u + \frac{\mathrm{i}K}{2}u \\
&\quad = \mathrm{i}\gamma\left(u|u|^2 + \frac{2}{3}u|v|^2 + \frac{1}{3}v^2u^*\right), \\
&\frac{\mathrm{d}v}{\partial z} - \frac{\Delta\beta_1}{2}\frac{\partial v}{\partial t} + \frac{\mathrm{i}\beta_2}{2}\frac{\partial^2 v}{\partial t^2} - \frac{\beta_3}{6}\frac{\partial^3 v}{\partial t^3} + \frac{\alpha}{2}u - \frac{\mathrm{i}K}{2}v \\
&\quad = \mathrm{i}\gamma\left(v|v|^2 + \frac{2}{3}v|u|^2 + \frac{1}{3}u^2v^*\right).
\end{aligned} \tag{1}$$

Here, u and v are the complex amplitudes of the desired field over different polarisation axes; $\Delta\beta_1$ is the difference in the inverse group velocities of pulses polarised along the slow and fast PM fibre axes; β_2 and β_3 are, respectively, the group-velocity and third-order dispersion coefficients; K is the linear-birefringence index; γ is a nonlinear factor; α is the linear loss coefficient; and z is the radiation propagation direction. The difference between the inverse group velocities $\Delta\beta_1$ and the linear-birefringence coefficient K in a PM fibre can be related as $\Delta\beta_1 = (\lambda/c)/(K/2\pi)$. In turn, $K = 2\pi/L_{\mathrm{beat}}$, where L_{beat} is the PM fibre beat length.

Equation (1) was solved by the split-step Fourier method [21]. The passive fibre was calculated using the following values of parameters: $\beta_2 = 20$ ps^2 km^{-1}, $\beta_3 = 0.04$ ps^3 km^{-1}, $\gamma = 5.5$ W^{-1} km^{-1}, and $L_{\mathrm{beat}} = 3$ mm. Generally, when considering PM fibres with a large birefringence index and, respectively, short beat length, one passes to the frame of reference of fibre polarisation modes and makes the following replacement of variables:

$$\begin{aligned}
u' &= u\exp(-\mathrm{i}Kz), \\
v' &= v\exp(\mathrm{i}Kz).
\end{aligned} \tag{2}$$

Due to this approach, the NSE is simplified, and one does not need to take a step less than L_{beat} in a numerical calculation. The last nonlinear term among the three ones in (1) is neglected as a product of slowly varying and rapidly oscillating functions. The simplified NSE has the form

$$\begin{aligned}
&\frac{\mathrm{d}u'}{\partial z} + \frac{\Delta\beta_1}{2}\frac{\partial u'}{\partial t} + \frac{\mathrm{i}\beta_2}{2}\frac{\partial^2 u'}{\partial t^2} - \frac{\beta_3}{6}\frac{\partial^3 u'}{\partial t^3} + \frac{\alpha}{2}u' \\
&\quad = \mathrm{i}\gamma\left(u'|u'|^2 + \frac{2}{3}u'|v'|^2\right), \\
&\frac{\mathrm{d}v'}{\partial z} - \frac{\Delta\beta_1}{2}\frac{\partial v'}{\partial t} + \frac{\mathrm{i}\beta_2}{2}\frac{\partial^2 v'}{\partial t^2} - \frac{\beta_3}{6}\frac{\partial^3 v'}{\partial t^3} + \frac{\alpha}{2}v' \\
&\quad = \mathrm{i}\gamma\left(v'|v'|^2 + \frac{2}{3}v'|u'|^2\right).
\end{aligned} \tag{3}$$

The calculation of the pulse evolution in active fibres is more difficult, because it calls for a description of the interaction with Yb^{3+} active ions. Within our model, this was done using a system of rate equations, with allowance for the interaction cross section. We considered the stationary case and assumed the population inversion to be settled:

$$\begin{aligned}
&\frac{\partial N_2 h\nu A_{\mathrm{eff}}}{\partial t} = 0 = GP_{\mathrm{p}}(\sigma_{\mathrm{a}}^{\mathrm{p}}N_1 - \sigma_{\mathrm{e}}^{\mathrm{p}}N_2) + P_{\mathrm{CW}}(\sigma_{\mathrm{a}}^{\mathrm{CW}}N_1 - \sigma_{\mathrm{e}}^{\mathrm{CW}}N_2) \\
&\qquad + \sum_j P_{\mathrm{s}}^j(\sigma_{\mathrm{a}}^{\mathrm{s}j}N_1 - \sigma_{\mathrm{e}}^{\mathrm{s}j}N_2) - \frac{h\nu A_{\mathrm{eff}}N_2}{\tau}, \\
&\frac{\partial P_{\mathrm{CW}}}{\partial z} = P_{\mathrm{CW}}(\sigma_{\mathrm{e}}^{\mathrm{CW}}N_2 - \sigma_{\mathrm{a}}^{\mathrm{CW}}N_1), \\
&\frac{\partial P_{\mathrm{s}}^j}{\partial z} = P_{\mathrm{s}}^j(\sigma_{\mathrm{e}}^{\mathrm{s}j}N_2 - \sigma_{\mathrm{a}}^{\mathrm{s}j}N_1), \\
&\frac{\partial P_{\mathrm{p}}}{\partial z} = GP_{\mathrm{p}}(\sigma_{\mathrm{e}}^{\mathrm{p}}N_2 - \sigma_{\mathrm{a}}^{\mathrm{p}}N_1), \\
&N_1 + N_2 = N.
\end{aligned} \tag{4}$$

Here, P_p, P_s^j, and P_{CW} are, respectively, the pump, pulsed signal, and cw radiation powers (with all spectral j components of signal radiation taken into account); σ_a^p, σ_a^{sj}, σ_a^{CW}, σ_e^p, σ_e^{sj}, and σ_e^{CW} are the absorption (subscript 'a') and stimulated emission (subscript 'e') cross sections for the pump radiation, pulsed signal, and cw radiation, respectively (the values are taken from [22] for ytterbium ions in silica fibres doped with P_2O_5); $A_{eff} = 33\ \mu m^2$ is the effective area of the signal mode in an active fibre; $\tau = 1.4$ ms is the lifetime of excited ytterbium ions; N_1 and N_2 are the concentrations of Yb^{3+} ions in the ground and excited states, respectively; $N = 13.24 \times 10^{22}\ cm^{-3}$ is the net concentration of ytterbium ions; and $G = 0.0013$ is the overlap integral of the multimode pump field with the active fibre core.

To relate the systems of equations (4) and (3), we applied the following expressions using the Fourier transform $F[f]$:

$$|F_j[u]|^2 \Delta\omega f = P_s^j,$$
$$F[\alpha] = -(\sigma_e^{sj} N_2 - \sigma_a^{sj} N_1), \quad (5)$$

where f is the pulse repetition frequency and $\Delta\omega$ is the frequency grid step.

In solving simultaneously the NSE and system of rate equations, the fibre was divided into segments so that the concentration of excited ions within each segment could be considered constant. The standard predictor–corrector method was applied to this end.

Raman scattering, which may be rather strong in passively mode-locked fibre lasers [23], was disregarded in our model. According to [21], the threshold peak pulse power at which this effect becomes pronounced is given by the expression

$$P_{th} \approx 16A/(Lg_R), \quad (6)$$

where $A = 33\ \mu m^2$ is the effective mode area in a passive fibre; L is the length of the medium; and $g_R \approx 10^{-13}$ m W^{-1} is the Raman gain in fused silica for a pump wavelength of 1 μm. The characteristic length of the cavity portion through which a pulse with the maximum peak power propagates does not exceed 3 m in the cases under consideration; therefore, the peak threshold power of optical pulses below which the model correctly describes the cavity operation is 1800 W. The calculated peak powers of the pulses generated in the cavities considered by us were no higher than this value.

According to [24, 25], the pulsed emission of a self-started passively mode-locked laser develops from noise in the case of cw laser operation. Therefore, when calculating the generation of pulses, it is important to take into account possible existence of cw radiation in the cavity. If the latter is disregarded in the model, one can obtain a steady-state pulse generation, which will be absent in practice [26]. In our model, jointly with the initial pulse, cw radiation was introduced into the cavity, and its evolution was calculated similarly to the pump radiation evolution. At each cavity round trip, the cw wavelength was corrected, assuming that it corresponds to the maximum product of gain and loss functions in the cavity.

3. Simulation results

The first set of important parameters determining the transmission function of a nonlinear element includes the angles δ_2 and δ_3 (see Fig. 1) between the PM fibre polarisation axes. The angle δ_3 was chosen to be equal to δ_2 in order to maximise the cw loss at a zero phase shift of the phase plate. The dependence of the transmittance on the input pulse peak power is such that at smaller input angles δ_2 the nonlinear element starts being more transparent at lower peak powers; in this case, however, the nonsaturating loss is higher than at larger angles (Fig. 2). This conclusion was substantiated in [20].

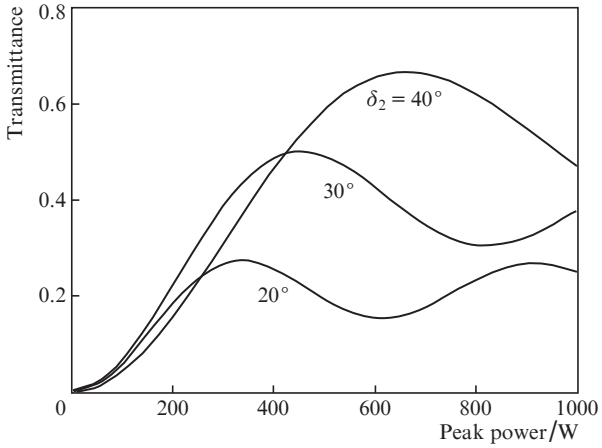

Figure 2. Dependence of the calculated transmittance of a 3-m nonlinear element on the peak power for a linearly chirped Gaussian pulse at input angles $\delta_2 = 20°$, 30°, and 40°; the output angle $\delta_3 = -\delta_2$.

The second, no less important, set of parameters of a nonlinear element includes the fibre lengths L_1 and L_2. The shorter these lengths, the higher the peak powers necessary for making the nonlinear element transparent. Correspondingly, pulses with a higher peak power (having a larger spectral width due to the fibre nonlinearity) will develop in a laser with a shorter nonlinear element. Therefore, after compensating for the linear chirp, one can reduce the pulse width, which is most interesting from the practical point of view. A simulation showed that the minimum values of fibre lengths L_1 and L_2 at which pulses can be generated is about 1.5 m in the proposed scheme. At these fibre lengths pulse generation is implemented at filter bandwidths in the range from 5 to 20 nm. The Gaussian filter bandwidth was chosen to be 15 nm.

To analyse in detail this cavity configuration, we calculated the stability zone: a region of space in the coordinates of phase shift $\Delta\varphi$ of the phase plate and pump power P_p, in which stable-amplitude pulses are generated. To calculate one point in this zone, 100 round trips were made. Figure 3 shows the calculated stability zone for the cavity configuration presented in Fig. 1. The instability of the peak pulse power for the last 15 cavity round trips is shown in colour. Generation of stable-amplitude pulses is absent in the white area but occurs in the dark red area. In all the points where generation of stable-amplitude pulses was observed, the cw component (present in the first round trip) decayed to a level below 10^{-20} W. The shape of a stationary optical pulse was independent of the initial pulse shape.

The peak power instability within the zone is 10^{-5}. The point at the centre of the stability zone corresponds to the configuration that is most stable against external effects; therefore, the most stable operation regime for the above-described configuration is obtained at an uncompensated birefringence corresponding to a phase shift $\Delta\varphi = 20°$.

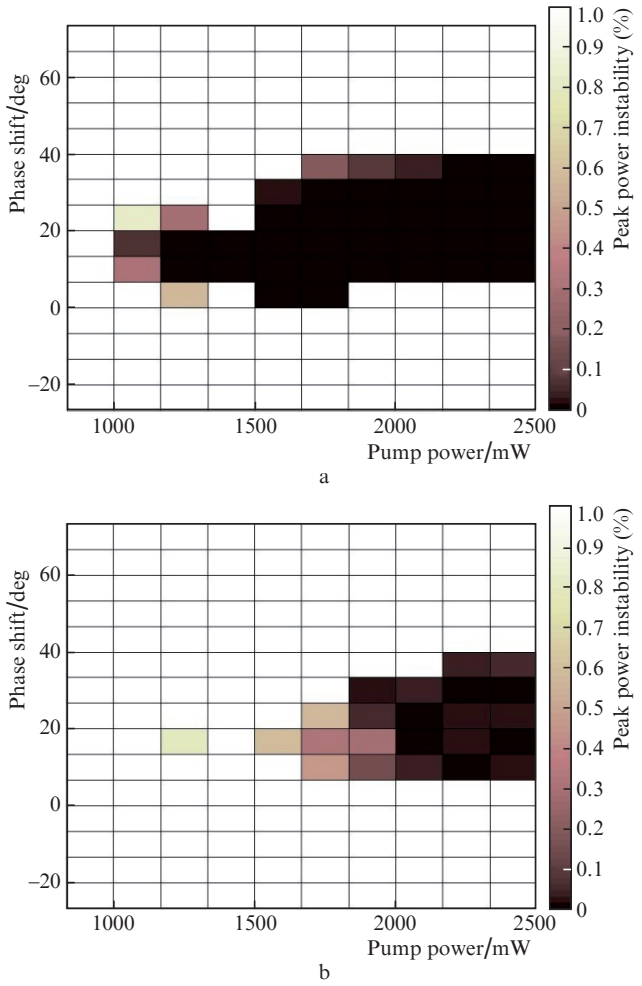

Figure 3. (Colour online) Stability zones calculated for the laser presented in Fig. 1 at δ_1 = (a) 90° and (b) 88°.

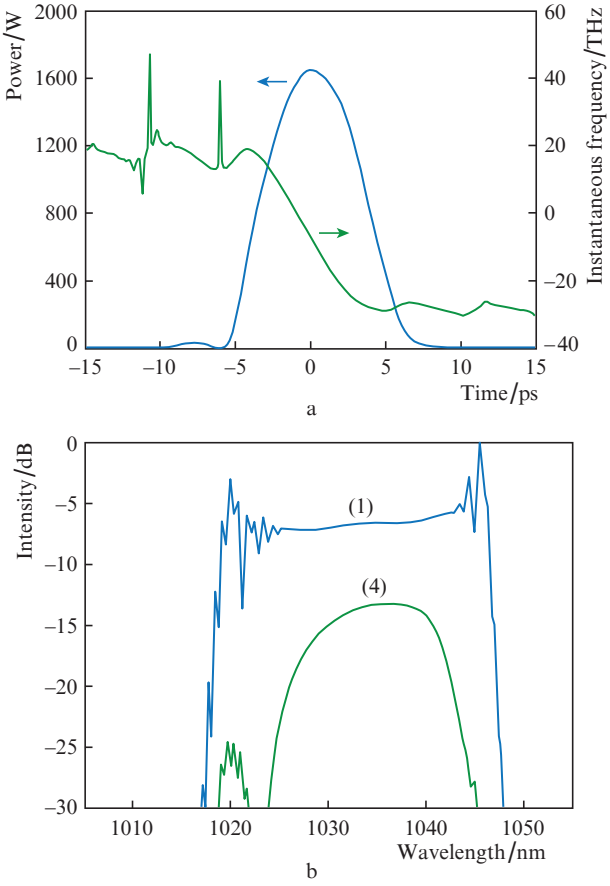

Figure 4. (a) Pulse shape and chirp at cavity point (1) and (b) the pulse spectra at cavity points (1) and (4) on the logarithmic scale. The pump power is P_p = 2200 mW and the phase shift is $\Delta\varphi$ = 20°.

The concept of stability zones can be used to analyse the laser scheme sensitivity against a change in some parameters of individual elements. For example, our simulation showed that the laser operation is very sensitive to the splicing of fibres with lengths L_1 and L_2, whose polarisation axes are rotated by an angle $\delta_1 = 90°$. The stability zone sharply decreases with a change in this angle by 2° (see Fig. 3b). A deterioration of the polarisation extinction for the radiation entering the nonlinear element also leads to a significant (but somewhat smaller) decrease in the stability zone, whereas deviations of angles δ_2 and δ_3 do not cause any significant changes in the stability zone.

The envelope, spectrum, and chirp of the pulses obtained using this scheme are presented in Fig. 4. The pulse energy at cavity point (1) (see Fig. 1) was 12 nJ. One can see that the output radiation contains a weak minor pulse (centred at about 8 ps), whose presence results in a spectral shape with irregular edges. Its occurrence is related to the group walk-off of the pulses with polarisations oriented along the fast and slow axes of PM fibre segments. If this walk-off is switched off in the model, the minor pulse disappears, as well as the irregularity on the spectrum edges.

The presence of a minor pulse is generally undesirable for master oscillators used as part of a more complex optical system. To implement generation of pulses with a wider spectrum and without a minor pulse, the fibre lengths L_1 and L_2 in the nonlinear element should be decreased. In addition, to implement generation of pulses on a maximally short nonlinear element, it must be located behind the active fibre, where the peak pulse power is maximum. One can also reduce the angle δ_2 between the PM fibre polarisation in order to decrease the peak power necessary for making the nonlinear element transparent. The corresponding optical scheme, obtained stability zone, and pulse parameters are presented in Fig. 5. In contrast to the pulses obtained with the scheme in Fig. 1, the generated pulses have a smoother spectrum, but their output energy is lower by a factor of 6.

It is of interest to compare our simulation results with the data of [9, 20], where a nonlinear element composed of several PM fibre segments was considered. Due to the presence of several segments with polarisation axes rotated by 90°, the propagating optical pulses with polarisations oriented along the fast and slow axes of PM fibre are constantly spatially overlapped, which results in a more symmetric transmission function without any minor maxima, as compared with a nonlinear element having two segments of the same length. However, this does not mean that a two-segment nonlinear element cannot be used for passive mode locking. The transmission function of a nonlinear element depends on not only the number of segments and their lengths but also the input pulse shape. This is demonstrated in Fig. 6, which presents the shapes and spectra of pulses transmitted through the nonlinear element used in the scheme in Fig. 1, at a zero phase shift of the phase plate. In all cases the input pulses had a peak

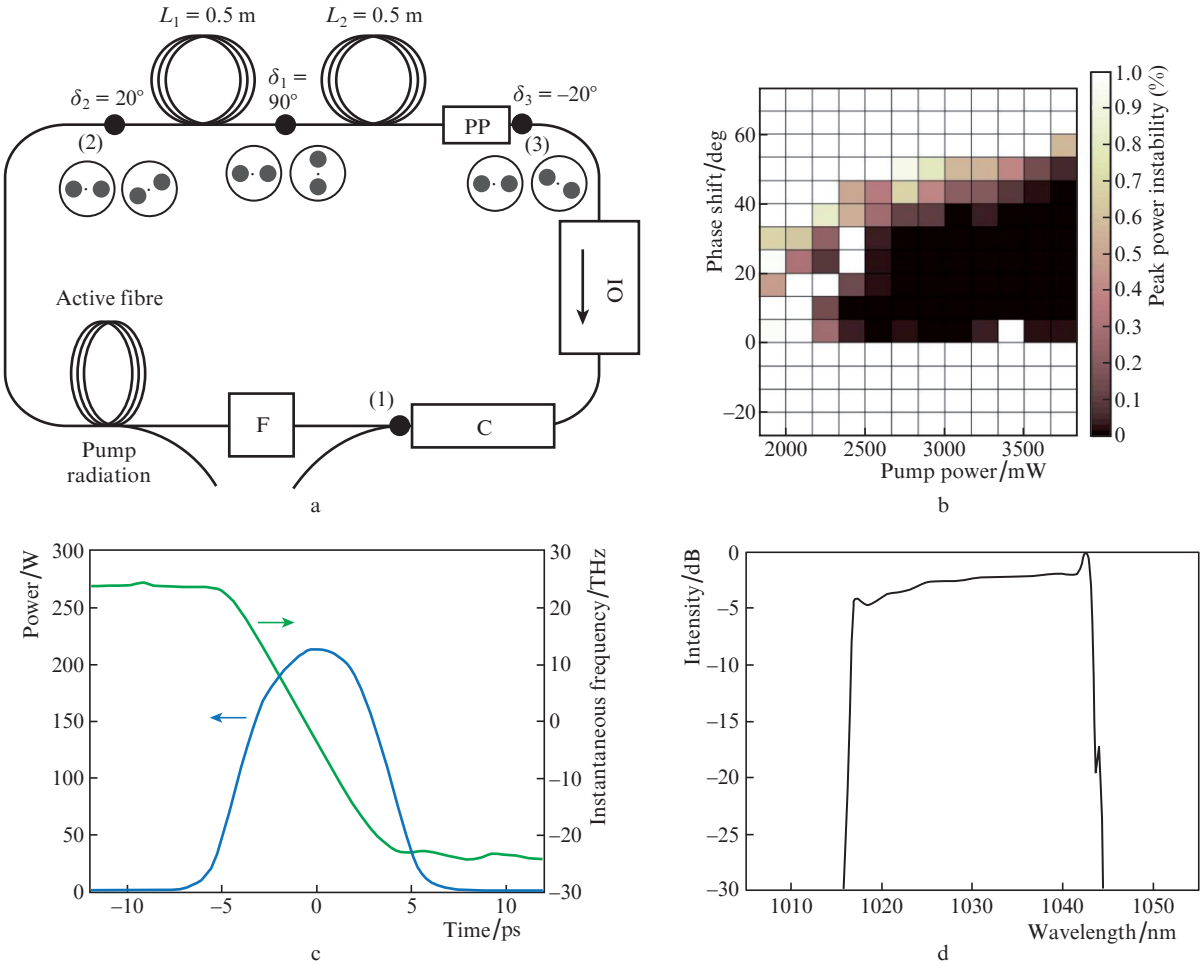

Figure 5. (Colour online) (a) Optical scheme with a nonlinear element located directly after the active fibre (the optical isolator OI is spliced with a polariser blocking the radiation polarised along the fast axis), (b) calculated stability zone, (c) pulse shape and chirp at cavity point (1) for P_p = 3500 mW and $\Delta\varphi = 30°$, and (d) pulse spectrum at point (1) for P_p = 3500 mW and $\Delta\varphi = 30°$.

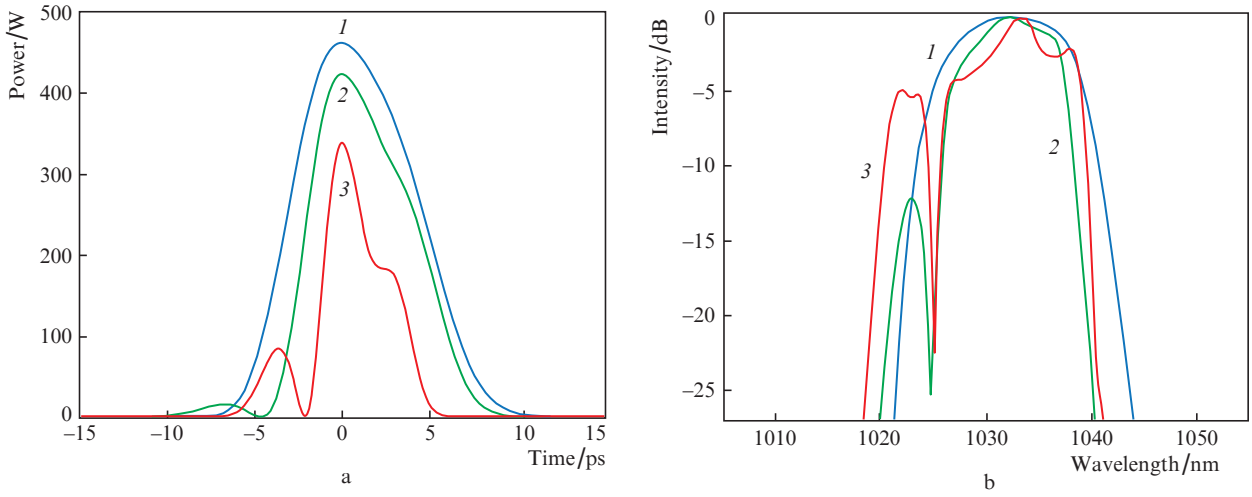

Figure 6. (a) Shapes and (b) spectra of pulses transmitted through the nonlinear element used in the scheme presented in Fig. 1. The FWHM values for the input pulse are (*1*) 15, (*2*) 8, and (*3*) 4 ps.

power of 1 kW and a spectral width of 9.4 nm at a level of 3 dB, they were linearly chirped and Gaussian-shaped, and their width varied from 15 to 4 ps. It can be seen that the 4-ps input pulse had significantly distorted shape and spectrum, whereas the longer pulses passed through the nonlinear element without such essential distortions. Therefore, from the

point of view of application of a nonlinear element in a passively mode-locked laser, it is important to consider its operation jointly with the parameters of the entire cavity.

In the case of the optical scheme shown in Fig. 1, the output pulse exhibited a minor peak and its spectrum was irregular because of the asymmetry of the nonlinear element transmission function. However, this peak disappeared when the walk-off of the pulses propagating with polarisations oriented along the PM fibre fast and slow axes was 'switched off' in the model. This is in complete agreement with the data of [20]. To obtain a pulse without a minor peak, the optical scheme of the cavity must be optimised so as to make the nonlinear element as short as possible. Therefore, the problem of generation of a short optical pulse with a smooth spectrum and without a minor peak can be solved either by optimising the length of a two-segment nonlinear element and other cavity parameters or using a nonlinear element consisting of three or more segments.

Thus, the concept of stability zones was used to investigate theoretically the scheme of a passively mode-locked laser based on the NPE effect in two PM fibre segments, spliced with rotation of the polarisation axes by an angle of 90°. The operation of this scheme is most stable when the uncompensated linear birefringence between the PM fibre segments is $\sim 20°$. It was found that the operating capacity of the scheme analysed is significantly affected by deviation of δ_1 (the splice angle of fibre polarisation axes) from 90°. It was also shown theoretically that, using a short nonlinear element, one can implement generation of linear chirped pulses with a spectral width of more than 25 nm at a wavelength of 1030 nm.

References

1. Dausinger F., Lichtner F. *Femtosecond Technology for Technical and Medical Applications* (Berlin: Springer Science & Business Media, 2004).
2. Osellame R., Cerullo G., Ramponi R. *Femtosecond Laser Micromachining: Photonic and Microfluidic Devices in Transparent Materials* (Berlin: Springer Science & Business Media, 2012).
3. Assion A. et al. *Science*, **282** (5390), 919 (1998).
4. Zheng Z., Iqbal M., Yu T. *Intern. J. Commun.*, **1** (3), 132 (2007).
5. Aguergaray C. et al. *Opt. Express*, **20** (10), 10545 (2012).
6. Matsas V.J. et al. *Electron. Lett.*, **28** (15), 1391 (1992).
7. Winters D.G. et al. *Opt. Express*, **25** (26), 33216 (2017).
8. Boivinet S. et al. *IEEE Photon. Technol. Lett.*, **26** (22), 2256 (2014).
9. Szczepanek Jan, Kardaś Tomasz M., Radzewicz Czesław, Stepanenko Yuriy. *Opt. Lett.*, **42**, 575 (2017).
10. Fermann M.E. et al. *Opt. Lett.*, **18** (11), 894 (1993).
11. Zhang W. et al. Opt. Express, **26** (7), 7934 (2018).
12. Leblond H. et al. *Phys. Rev. A.*, **65** (6), 063811 (2002).
13. Haus H.A., Fujimoto J.G., Ippen E.P. *JOSA B*, **8** (10), 2068 (1991).
14. Haus H.A., Fujimoto J.G., Ippen E.P. *IEEE J. Quantum Electron.*, **28** (10), 2086 (1992).
15. Martinez O.E., Fork R.L., Gordon J.P. *Opt. Lett.*, **9** (5), 156 (1984).
16. Kuizenga D., Siegman A. *IEEE J. Quantum Electron.*, **6** (11), 694 (1970).
17. Baranov A.I., Myasnikov D.V. *Proc. Laser Optics, 2014 Intern. Conf.* (Saint Petersburg: IEEE, 2014) p.1-1.
18. Liu X. *Opt. Express*, **17** (25), 22401 (2009).
19. Tang D.Y. et al. *Phys. Rev. A*, **72** (4), 043816 (2005).
20. Szczepanek J., Kardaś T.M., Radzewicz C., Stepanenko Y. *Opt. Express*, **26** (10), 13590 (2018).
21. Agrawal G.P. *Nonlinear Fiber Optics* (New York: Rochester, 1996).
22. Mel'kumov M.A., et al. *Quantum Electron.*, **34** (9), 843 (2004) [*Kvantovaya Elektron.*, **34** (9), 843 (2004)].
23. Bednyakova A.E., Babin S.A., Kharenko D.S., Podivilov E.V., Fedoruk M.P., Kalashnikov V.L., Apolonski A. *Opt. Express*, **21**, 20556 (2013).
24. Krausz F., Brabec T., Spielmann C. *Opt. Lett.*, **16** (4), 235 (1991).
25. Chen C.J., Wai P.K.A., Menyuk C.R. *Opt. Lett.*, **20** (4), 350 (1995).
26. Protasenya D.V., Baranov A.I., Myasnikov D.V. *Proc. Laser Optics, 2016 Intern. Conf.* (Saint Petersburg: IEEE, 2016) p. S1-5.